

Field Fluctuation Spectroscopy in a Reverberant Cavity with Moving Scatterers

Julien de Rosny,* Philippe Roux, and Mathias Fink

Laboratoire Ondes et Acoustique, ESPCI, Université Paris VII, U.M.R. 7587 C.N.R.S., 10 rue Vauquelin, 75005 Paris, France

J. H. Page

Department of Physics and Astronomy, University of Manitoba, Winnipeg, Manitoba, Canada, R3T 2N2

(Received 28 November 2002; published 6 March 2003)

We report a study of transient ultrasonic waves inside a reverberant cavity containing moving scatterers. We show that the elastic mean free path and the dynamics of the scatterers govern the evolution of the autocorrelation of acoustic wave field. A parallel is established between these results and a closely related technique, diffusing acoustic wave spectroscopy. Excellent agreement is found between experiment and theory for a moving stainless steel ball in a water tank, thereby elucidating the underlying physics, and a potential application, fish monitoring inside aquariums, is demonstrated.

DOI: 10.1103/PhysRevLett.90.094302

PACS numbers: 43.35.+d, 43.20.+g, 43.80.+p, 43.90.+v

The propagation of waves in complex media has attracted renewed interest over the past two decades. Many studies have focused on wave phenomena associated with strong multiple scattering and their interpretation based on the diffusion approximation [1]. This has led to the development of new techniques to probe diffusive media where traditional methods based on the single scattering approximation fail. For example, diffusing wave spectroscopy (DWS) in optics [2,3] and diffusing acoustic wave spectroscopy (DAWS) in acoustics [4] have shown how the dynamics of moving scatterers can be measured from the fluctuations of the multiply scattered intensity and field. Another family of complex propagation phenomena is being extensively studied in closed cavities with reverberant boundaries (quantum dots, chaotic billiards, reverberant rooms, ...). In such media, the wave field is “diffuse” for an entirely different reason: because of multiple reflections at the boundaries, the wave field fills the cavity and becomes isotropic and homogeneous on average. Thus, the field is diffuse in the sense of room acoustics theory [5]. When the medium inside the cavity is heterogeneous, waves can be both scattered from the inhomogeneities and reflected by the boundaries, leading to a rich interplay of multiple scattering and multiple reflection effects even when the scattering is relatively weak [6]. However, when the scatters are static, it is difficult to unravel this interplay, as the wave propagation differences between an empty cavity and one filled with weak scatterers can be very small. This observation motivates a question that has not been addressed previously apart from one preliminary study [7]: what happens when the scatterers inside a reverberant cavity are moving? The answer to this question is potentially important, not only because it may provide a new way of learning about the mixing of two kinds of wave physics, but also because it could lead to a new way of probing the dynamics of scatterers in complex media.

In this Letter, we address this problem experimentally and theoretically using ultrasonic waves. Unlike DAWS,

the experiments are conducted in a reverberant water tank containing relatively few scatterers, so that the mean free path is large compared to the cavity dimensions. In this regime, we show that the diffuse nature of the wave field due to boundary reflections allows wave scattering to be described in relatively simple terms: the energy transfer between the different scattering orders is a Markoff-Poisson process that depends on the elastic mean free time. Furthermore, the fact that the spatial correlations of the wave field are governed by the cavity and not by the scatterers allows a simple form for the field autocorrelation function to be derived. We show that the autocorrelation depends on both the scattering mean free path and the dynamics of the scatterers, opening up a new technique in field fluctuation spectroscopy which we call diffusing reverberant acoustic wave spectroscopy. The sensitivity of the technique to scatterer motion is governed by the condition that the autocorrelation reaches its minimum when the scatterers have moved by λ/\sqrt{m} , where λ is the wavelength and m is the scattering order. These predictions are demonstrated experimentally through a series of experiments in which the motion of a stainless steel ball inside a water tank is fully controlled by stepping motors. Excellent agreement is found between theory and experiment both for measurements of the mean free path and for the autocorrelation evolution for two different kinds of motion: ballistic (straight trajectories) and diffusive (random walks). Finally, we discuss a potential application: fish monitoring inside an aquarium.

In a reverberant cavity with scatterers, the time dependence of the pressure wave field, $\phi(t)$, can be decomposed into an infinite sum of $\phi_m(t)$ wave fields. Here $\phi_m(t)$ represents the wave field which is scattered m times, and t is the propagation time of the wave after its emission from the source (at $t = 0$). As explained above, the fields $\phi_m(t)$ are diffuse. In this case, the mean energy density $\langle \epsilon_m \rangle$ of the m th scattered wave field is equal to $\langle \phi_m^2 \rangle / \rho_0 c^2$, where c is the sound speed and ρ_0 is the mass density of the propagation medium. Here we assume that the cloud

of scatterers is dilute, and, therefore, there is no correlation between the fields scattered by the different particles. Between times t and $t + dt$, the total energy $V\langle\epsilon_m\rangle$ decreases by $N\langle\epsilon_m\rangle\sigma_s c dt$ due to scattering by the N scatterers, where σ_s is the total elastic scattering cross section and V is the volume of the cavity. At the same time, for wave fields scattered at least once, $V\langle\epsilon_m\rangle$ increases by $N\langle\epsilon_{m-1}\rangle\sigma_s c dt$ due to the contribution of the $(m-1)$ th scattered fields. In terms of mean squared fields, a Kolmogoroff set of equations is obtained:

$$\begin{aligned} d\langle\phi_0^2(t)\rangle/dt &= -\langle\phi_0^2(t)\rangle/\tau_s, \\ d\langle\phi_m^2(t)\rangle/dt &= (\langle\phi_{m-1}^2(t)\rangle - \langle\phi_m^2(t)\rangle)/\tau_s, \quad m \geq 1, \end{aligned} \quad (1)$$

where the time τ_s is equal to $V/N\sigma_s c$. This set of equations is characteristic of a Markoff-Poisson process, whose solution $\langle\phi_m^2(t)\rangle$ is $\langle\phi_0^2(0)\rangle e^{-t/\tau_s} (t/\tau_s)^m / m!$. Note that the total intensity that is not scattered, $\langle\phi_0^2(t)\rangle$, is simply equal to $\langle\phi_0^2(0)\rangle e^{-t/\tau_s}$ and decreases exponentially with distance traveled according to the magnitude of the elastic scattering mean free path, ℓ_s ($\ell_s = c\tau_s$). Moreover, the fraction of the wave field that has been scattered m times, $\langle\phi_m^2(t)\rangle/\langle\phi_0^2(0)\rangle$, is a maximum at the time $t = m\tau_s$. When the incident field is pulsed, the evolution of the field due to the motion of the scatterers can be observed, at all propagation times t , by measuring the transient fields on subsequent repetitions of the pulse. Thus, the influence of the motion of the scatterers on the autocorrelation of the field, $\langle\phi^{\{T_1\}}(t)\phi^{\{T_2\}}(t)\rangle$, can be determined at any propagation time t . Here $\phi^{\{T_1\}}(t)$ and $\phi^{\{T_2\}}(t)$ are the transient pressure fields at times T_1 and T_2 . Since the time scale of acoustic wave propagation t is much faster than the time scale for the scatterers to move a detectable distance, $\Delta T = T_2 - T_1$ (i.e., low Mach number), the medium can be considered “frozen” for all t , as in DAWS and DWS. Then $\langle\phi^{\{T_1\}}(t)\phi^{\{T_2\}}(t)\rangle$ can be rewritten as $\langle\phi^{\{0\}}(t)\phi^{\{\Delta T\}}(t)\rangle$, and the dependence of the autocorrelation function on acoustic propagation time t and scatterer motion time ΔT become decoupled. Moreover, between two scattering events, the wave field is completely randomized by multiple reflections at the cavity boundaries, so that the scattered pressure fields for different m are uncorrelated, i.e., $\langle\phi_m\phi_{m+1}\rangle = 0$. Hence,

$$\langle\phi^{\{0\}}(t)\phi^{\{\Delta T\}}(t)\rangle = \sum_{m=0}^{\infty} \langle\phi_m^{\{0\}}(t)\phi_m^{\{\Delta T\}}(t)\rangle. \quad (2)$$

Generally speaking, the calculation of each term of the right-hand side of Eq. (2) is quite complex. However, it can be shown that for a single moving scatterer the normalized autocorrelation function of the m th scattered field, $g_1^{(m)}(\Delta T) = \langle\phi_m^{\{0\}}(t)\phi_m^{\{\Delta T\}}(t)\rangle/\langle\phi_m^2(t)\rangle$, is

$$g_1^{(m)}(\Delta T) = \int_0^{\infty} C^m(\Delta r) \mathcal{P}_{\Delta T}(\Delta r) d\Delta r. \quad (3)$$

Here $\mathcal{P}_{\Delta T}(\Delta r)$ is the probability for one particle to move by Δr within time ΔT , and $C(\Delta r)$ is the normalized spatial autocorrelation function of the wave field that is scattered once. It is well known in room acoustics and wave chaos that the spatial autocorrelation of a field with wave number k in the diffusive regime is given by $\sin(k\Delta r)/k\Delta r$ [8]. Hence, $C(\Delta r)$ is equal to $\text{sinc}^2(k\Delta r)$. The square accounts for the double process involved for one scattering event: reception and emission. In Eq. (3), $C(\Delta r)$ is raised to the m th power since the wave field is decorrelated by the factor $C(\Delta r)$ for each scattering event. Notice also that $g_1^{(m)}(\Delta T) = 1$ for $m = 0$. Finally, the normalized correlation function of the complete wave field, $g_1^{(i)}(\Delta T) = \langle\phi^{\{0\}}(t)\phi^{\{\Delta T\}}(t)\rangle/\langle\phi^2(t)\rangle$, is

$$g_1^{(i)}(\Delta T) = e^{-t/\tau_s} \left[1 + \sum_{m=1}^{\infty} \frac{(t/\tau_s)^m}{m!} g_1^{(m)}(\Delta T) \right]. \quad (4)$$

Hence, for a fixed propagation time or path length of the diffusing sound in the cavity, the autocorrelation function is composed of a constant term, e^{-t/τ_s} , and additional terms that decrease with the scatterer displacement within ΔT . Moreover, the characteristic decay time of $g_1^{(i)}(\Delta T)$ at fixed t is the time needed for the particles to move by roughly $1/k\sqrt{m}$ [since $C^m(\Delta r) \cong \exp(-mk^2\Delta r^2/3)$]. Until now, absorption has not been considered. However, as in DAWS, absorption does not contribute to $g_1^{(i)}(\Delta T)$ for measurements at fixed t , as its effects cancel out in the normalization of the autocorrelation function.

In order to definitively test this model of the transient behavior of the wave fields, experiments were set up in which the scatterer motion was completely controlled. The reverberant cavity was a thin stainless steel tank filled with about 1.6 liters of water. Bumps were made on the cavity boundary to quickly spread the wave over the entire cavity volume and reach a diffuse regime. The emitter and the receiver were 400 kHz transducers with a 30% bandwidth. The scatterer was a stainless steel 19-mm-diameter sphere, which was immersed in the water and attached to a two-axis stepping motor system located above the water surface. Thanks to the stepping motors, the ball trajectory could be decomposed into small straight segments. A typical experiment was performed as follows. Here a straight (or ballistic) trajectory is illustrated: all the small straight segments were aligned. The length of a segment was 200 μm and there were 49 segments. Between adjacent segments, the transient field $\phi^{(\eta)}(t)$ was recorded. For convenience, the time ΔT has been replaced by the segment index η ($0 < \eta < 49$). In order to have an accurate measurement of the autocorrelation, the $\phi^{\{0\}}(t)\phi^{\{\eta\}}(t)$ product was integrated over a small propagation time window (the window width was 100 μs , which is short compared to the 1 ms mean free time). Moreover, the measurements were averaged over ten different trajectories, where for each trajectory,

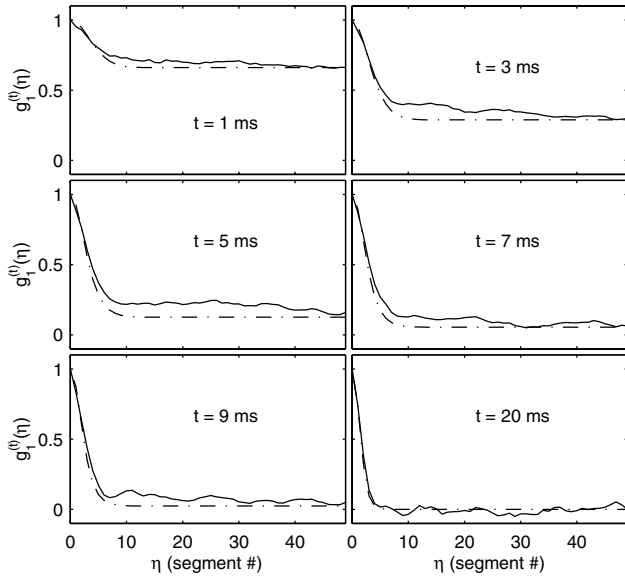


FIG. 1. Six evolutions of the correlation function with respect to η (segment number) for ballistic motion of a 19-mm-diameter ball (solid curves, experiment; dot-dashed curves, theory). The segment length was 0.2 mm.

the origin of the ball (position at $\eta = 0$) and the initial displacement direction were chosen at random. The normalized autocorrelation functions are plotted in Fig. 1. As expected, the correlation is the sum of two contributions: a constant plateau (due to the unscattered wave field) and decreasing terms (related to the ball displacement). The plateau level decreases with t .

First, we focus briefly on the plateau. In order to have a better estimation of the plateau level, the autocorrelation was measured from 100 positions of the 19-mm-diameter ball for which the distance between two positions was larger than 10 mm. As predicted theoretically, a nice decreasing exponential is found (see Fig. 2). The experiments were repeated with two other balls having diameters of 17 and 25 mm, respectively. From the slopes, the mean free paths and total cross sections were deduced (see Table I). The experimental cross sections correspond well to theoretical predictions [9]. Demer *et al.* have extended this study to the frequency dependence of the total cross section [9].

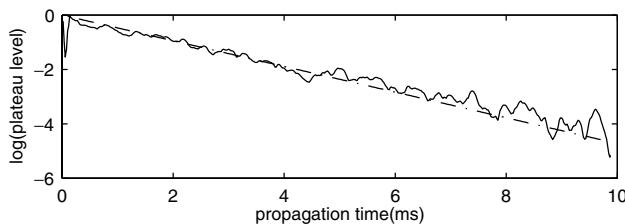


FIG. 2. Evolution of the plateau level with propagation time t for the 19-mm-diameter ball (continuous line). The dashed line represents an exponential fit.

TABLE I. Comparison between experimental and theoretical total cross sections for stainless balls of different diameters.

Ball diam. (mm)	17	19	25
Exp. mean free path (m)	4.53	3.18	1.86
σ_s exp. (mm ²)	353	510	860
σ_s theor. (mm ²)	370	500	865

Next, we focus on the dynamic part of the autocorrelation. In order to better resolve the decay of the autocorrelation function, an experiment was performed with the 19-mm-diameter ball using a shorter 40 μ m segment length (see Fig. 3). For ballistic motion with segment lengths δx [$\mathcal{P}_\eta(\Delta r) = \delta(\Delta r - \eta\delta x)$], Eq. (3) gives $g_1^{(m)}(\eta) = \exp(-mk^2\eta^2\delta x^2/3)$. Substituting this expression into Eq. (4) gives the dot-dashed curves in Figs. 1 and 3 (left side), in very good agreement with the experimental results. The opposite of ballistic motion is a random walk. Here, due to the two-axis motors, the random walk was investigated experimentally in two dimensions. The random walk consisted of 49 segments, each 0.2 mm long, with the directions of all the segments picked at random. A 2D random walk is a diffusive motion with a diffusion constant D equal to $\delta x^2/4$. In this case, Eq. (3) gives $1/(1 + 4mk^2D\eta/3)$. Again when this result is substituted in Eq. (4) and summed over all m , very good agreement is found between theory and experiment, as shown in the right side of Fig. 3.

An important parameter is the characteristic width, w_η , of $g^{(i)}(\eta)$. w_η decreases faster for diffusive motion ($w_\eta \approx 1/mk^2D$) than for ballistic motion ($w_\eta \approx 1/k\delta x\sqrt{m}$). This behavior is clearly observed in the experimental results (see Fig. 4).

To illustrate one of the many possible applications of these results, we show how they can be used to monitor fish inside an aquarium. Here the fish are the moving scatterers and the aquarium is the reverberant cavity. A

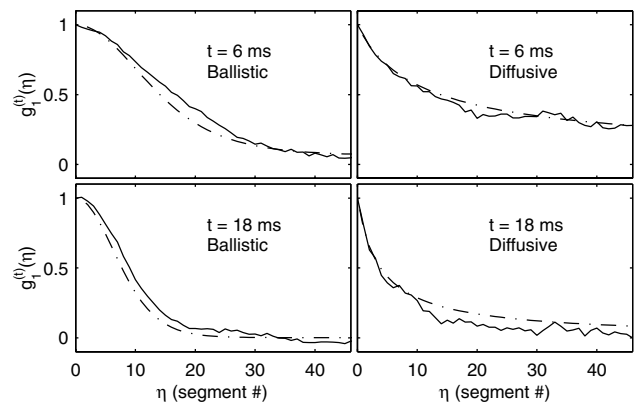


FIG. 3. The autocorrelation functions (solid curves, experiment; dot-dashed curves, theory) at $t = 6$ ms and $t = 18$ ms for ballistic motion (0.04 mm segment length) and diffusive motion (0.20 mm segment length).

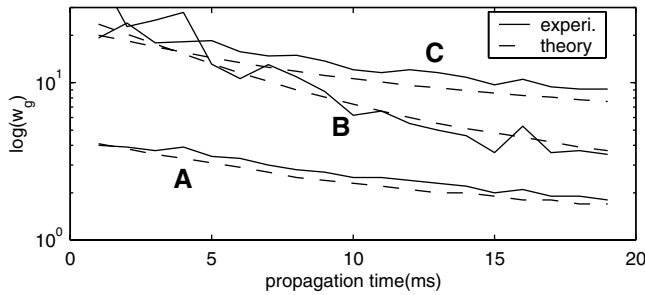


FIG. 4. Evolution of the width at half-maximum of the autocorrelation function with respect to the propagation time t . Curves A and C correspond to ballistic motions with step lengths of 0.20 and 0.04 mm, respectively. Curve B corresponds to a random walk with a 0.20 mm step length.

demonstration experiment was performed with four 30-mm-long fish inside a 0.55-liter aquarium. The same 400 kHz transducers were used. From the plateau in g_1 , a mean free time of 1.81 ms was found, corresponding to a scattering cross section per fish of 51 mm². In Fig. 5, the autocorrelation function at $t = 3$ ms is plotted. To interpret these data, Eq. (3) must be modified to account for the presence of several scatterers whose motions can be considered independent. In the limit of a large number of scatterers compared to the scattering order m , $g_1^{(m)}(\Delta T)$ is equal to $(\int_0^\infty C(\Delta r)\mathcal{P}_{\Delta T}(\Delta r)d\Delta r)^m$. At the earliest times, the experimental autocorrelation function appears to have negative curvature (see Fig. 5), suggesting that the motion is ballistic (cf. Fig. 3). Even though the resolution is rather poor, a ballistic fit with a fish speed of 15 mm/s seems to be consistent with the data. At longer times, the curve has opposite curvature, and a 3D random walk with $D = 0.70$ mm²/s gives an excellent fit to the experimental data. The 0.14 mm mean free path of the fish motion that is extracted from these two quantities is remarkably small. In fact, fish are very complex scatterers: they are anisotropic and can rotate, and their shape changes as they move. All these effects accelerate a lot the decay of the autocorrelation function and therefore reduce the fish mean free path.

In conclusion, we have used ultrasonic waves to investigate the fluctuations of the wave field due to the motion of scatterers inside a static reverberant cavity. We have also developed a theory, in the limit of large scattering mean free path compared to the largest cavity dimension, that gives an excellent description of the experimental results, thus elucidating the physics of wave propagation under these conditions. By showing how the field autocorrelation function depends on the scattering mean free

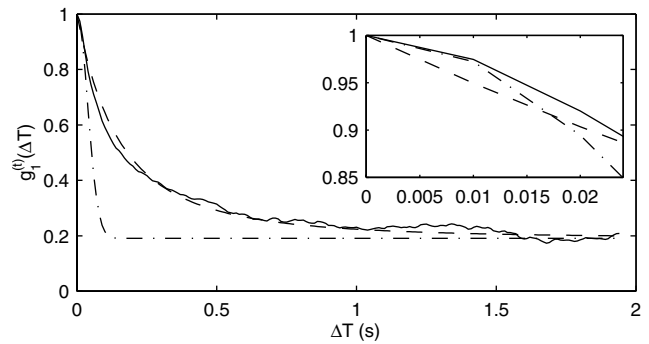


FIG. 5. Autocorrelation function recorded for four zebra fishes. The solid line corresponds to experimental data, the dashed curve is a fit to the theory for 3D diffusive motion with $D = 0.70$ mm²/s, and the dot-dashed curve is a fit to ballistic motion with $v = 15$ mm/s. The inset zooms in on the behavior at early times.

path of the waves and motion of the scatterers, we have demonstrated the principles of a new technique in field fluctuation spectroscopy, diffusing reverberant acoustic wave spectroscopy (DRAWS). Since waves in reverberant media play an important role not only in acoustics but in other areas of physics (e.g., in quantum dots and chaotic cavities), the range of potential applications of these results may be very wide.

We thank Arnaud Derode and Arnaud Tourin for useful discussions.

*Electronic address: julien.derosny@espci.fr
<http://www.loa.espci.fr/~julien>

- [1] P. Sheng, *Introduction to Wave Scattering, Localization, and Mesoscopic Phenomena* (Academic Press, San Diego, 1995).
- [2] D. J. Pine, D. A. Weitz, P. M. Chaikin, and E. Herbolzheimer, *Phys. Rev. Lett.* **60**, 1134 (1988).
- [3] G. Maret and P. E. Wolf, *Z. Phys. B* **65**, 409 (1987).
- [4] M. L. Cowan, J. H. Page, and D. A. Weitz, *Phys. Rev. Lett.* **85**, 453 (2000); M. L. Cowan, I. P. Jones, J. H. Page, and D. A. Weitz, *Phys. Rev. E* **65**, 066605 (2002).
- [5] M. Schroeder, *J. Acoust. Soc. Am.* **31**, 1407 (1959).
- [6] R. L. Weaver and D. Sornette, *Phys. Rev. E* **52**, 3341 (1995).
- [7] J. de Rosny and P. Roux, *J. Acoust. Soc. Am.* **109**, 2587 (2001).
- [8] R. Cook, R. Waterhouse, R. Berendt, S. Edelman, and M. Thompson, *J. Acoust. Soc. Am.* **27**, 1072 (1955).
- [9] D. Demer, S. Conti, J. de Rosny, and P. Roux, *J. Acoust. Soc. Am.* **113**, 1387–1394 (2003).